Research Square

Preprints are preliminary reports that have not undergone peer review.
They should not be considered conclusive, used to inform clinical practice,
or referenced by the media as validated information.

High-resolution ODMR spectra of individual hybrid 14 NV- 13 C spin systems with third-shell 13 C in diamond for nanoscale vector magnetometry: Theory and experiment

A. P. Nizovtsev

a.nizovtsev@ifanbel.bas-net.by

B.I. Stepanov Institute of Physics

A. L. Pushkarchuk

Institute of Physical and Organic Chemistry of the National Academy of Sciences of Belarus

N. S. Kukin

National Research Nuclear University MEPhI

A. R. Muradova

National Research Nuclear University MEPhI

A. K. Nikitin

National Research Nuclear University MEPhI

A. A. Bukhtiyarov

ANO "Institute of Engineering Physics"

P. A. Semenov

National Research Nuclear University MEPhI

V. G. Sukharev

ANO "Institute of Engineering Physics"

A. N. Vasiliev

National Research Nuclear University MEPhI

S. Ya. Kilin

National Academy of Sciences of Belarus

Research Article

Keywords: Diamond, single NV center, 13C nuclear spin, optically detected magnetic resonance, vector magnetometry, nanoscale

Posted Date: May 22nd, 2026

DOI: https://doi.org/10.21203/rs.3.rs-9607211/v1

License: This work is licensed under a Creative Commons Attribution 4.0 International License.
Read Full License

Additional Declarations: No competing interests reported.

Version of Record: A version of this preprint was published at Applied Magnetic Resonance on July 1st, 2026. See the published version at https://doi.org/10.1007/s00723-026-01847-7.

High-resolution ODMR spectra of individual hybrid ^{14}NV-^{13}C spin systems with third-shell ^{13}C in diamond for nanoscale vector magnetometry: Theory and experiment

A.P. Nizovtsev[1,2]*, A.L. Pushkarchuk[2,3], N.S. Kukin[2,4], A.R. Muradova[2,4], A.K. Nikitin[2,4], A.A. Bukhtiyarov[4], P.A. Semenov[2], V.G. Sukharev[4], A.N. Vasiliev[2], S.Ya. Kilin[1,2]

[1]Institute of Physics of the National Academy of Sciences of Belarus, 220072, Minsk, Belarus.
[2]National Research Nuclear University MEPhI, 115409, Moscow, Russia.
[3]Institute of Physical-Organic Chemistry of the National Academy of Sciences of Belarus, 220072, Minsk, Belarus.
[4]ANO "Institute of Engineering Physics", 142210, Serpukhov, Moscow Region, Russia.

*e-mail: a.nizovtsev@ifanbel.bas-net.by

Abstract

In recent decades, second-generation quantum technologies based on the practical use of individual quantum systems—atoms, molecules, impurity centers, and photons—have become one of a central focus of modern science. Among these, *quantum magnetometry* has emerged as one of the most advanced directions. In this field, nitrogen–vacancy (NV) centers in diamond, as well as their complexes with nuclear spins, are widely employed as sensors for measuring magnetic fields with nanometer-scale spatial resolution. However, due to the C_{3v} symmetry of the NV center, information about the azimuthal angle of the magnetic field vector is not accessible. Here, we propose and experimentally demonstrate, for a first time, a method of vector magnetometry based on acquisition and theoretical analysis of high-resolution optically detected magnetic resonance (ODMR) spectra of an *individual hybrid electron-nuclear three-spin system ^{14}NV-^{13}C*, in which the electron spin of a single NV center is coupled by hyperfine interaction with the intrinsic nuclear spin of the ^{14}N atom of the center as well as with the spin of *the isotopic atom ^{13}C, located in the third coordination sphere of the NV center.*

Key words: Diamond, single NV center, ^{13}C nuclear spin, optically detected magnetic resonance, vector magnetometry, nanoscale.

1 Introduction

In recent decades, the development of second-generation quantum technologies based on the practical use of *individual* quantum systems— atoms, molecules, impurity centers, and photons—has become one of a central focus of modern science [1]. One of the most advanced areas in this field is *quantum magnetometry,* in which nitrogen–vacancy (NV) centers in diamond, as well as their complexes with nuclear spins, are widely used as sensors for measuring magnetic fields with nanometer-scale spatial resolution [2]. The physical basis of such nanoscale magnetometry lies in the sensitivity of the ground-state triplet ($^3A_2$) sublevels of the NV center to external magnetic fields. The magnetic field shifts and mixes the sublevels corresponding to different projections of the electron spin (m_s = 0, ±1). These changes are typically detected using confocal microscopy in combination with optically detected magnetic resonance (ODMR), which provides an increase in sensitivity of up to ~7 orders of magnitude compared to conventional electron paramagnetic resonance (EPR) techniques. Theoretical analysis of ODMR spectra enables *vector magnetometry*, i.e., the quantitative determination of both the magnitude B of the local magnetic field and its orientation, defined in a spherical coordinate system by the polar θ and the azimuthal φ angles.

Currently, most vector magnetometers rely on recording and analyzing ODMR spectra of NV ensembles with orientations distributed among the four crystallographic axes of the diamond lattice. In such sensors, the spatial resolution is limited by the separation between individual centers, which typically ranges from tens to hundreds of nanometers. In contrast, *single NV centers offer maximal spatial resolution*. However, in this case, the ODMR transition frequencies ($m_s = 0 \leftrightarrow m_s = \pm 1$) depend only on the magnetic field strength B and the polar angle θ, due to the axial C_{3v} symmetry of the NV center, while information about the azimuthal angle φ is lost.

To overcome this limitation, a method of complete vector magnetometry based on *individual hybrid electron–nuclear spin systems* has been proposed in [3]. Instead of a single NV center, it was proposed to use a hybrid electron-nuclear complex consisting of a single NV center coupled via hyperfine interaction (*hfi*) to the nearby ^{13}C nuclear spin. The resulting ^{14}NV–^{13}C complex has lower C_S symmetry, and its high-resolution ODMR spectrum contains complete information about the magnetic field parameters B, θ, and φ. This approach was experimentally demonstrated in [4,5] for the ^{14}NV–^{13}C system in which the ^{13}C atom occupies the nearest-neighbor position relative to the NV center vacancy, corresponding to the strongest hyperfine interaction with the electronic spin of the center.

Subsequently, in [6], a similar approach to vector magnetometry was developed for more general NV–^{13}C systems with arbitrary configurations [6]. In that work, the method relied on measuring ODMR line frequencies and analyzing them using prior knowledge of hyperfine interaction parameters obtained from quantum chemical calculations [7]. Experimental verification in [6] was carried out for a system in which the ^{13}C atom was located in the third

coordination shell of the NV center. However, the use in [6] of a low-purity diamond sample resulted in relatively broad ODMR lines (~5 MHz), which prevented the observation of fine spectral features [3] responsible for extracting information about the azimuthal angle φ.

Recently, a high-quality single-crystal diamond sample with a chemically pure chemical-vapor-deposition (CVD) layer was synthesized at the Technological Institute for Superhard and Novel Carbon Materials [8]. In this sample, individual NV centers exhibit high-resolution ODMR spectra with linewidths as narrow as ~180 kHz [9], allowing clear resolution of hyperfine structure associated with the interaction between the NV electron spin and the intrinsic ^{14}N nuclear spin. In addition, various hybrid ^{14}NV-^{13}C spin systems were identified by analyzing their ODMR spectra in the absence of external magnetic field and comparing them with quantum-chemical predictions [7]. Among them, previously studied complexes ^{14}NV-^{13}C, involving ^{13}C atoms in the third coordination shell, were discovered. In the present work, we take the next step by demonstrating vector magnetometry based on high-resolution ODMR spectra of such individual hybrid spin systems. We report a combined theoretical and experimental study of a ^{14}NV–^{13}C(third-shell) system, enabling the determination of the magnitude and orientation (B, θ, φ) of an initially unknown local magnetic field. These results provide the first experimental evidence of the applicability of such systems for nanoscale vector magnetometry.

2 Theoretical methods and experimental part

For theoretical modeling of ODMR spectra of an arbitrary hybrid spin system ^{14}NV-^{13}C in an external magnetic field $\boldsymbol{B}$, we use the standard spin-Hamiltonian (see, e.g. [7])

$$H = H_0^{(NV)} + \boldsymbol{S}\cdot A^{(C)}\cdot \boldsymbol{I}^{(C)} + \beta_e g^{(NV)} \boldsymbol{S}\cdot\boldsymbol{B} - \beta_n g_n^{(N)} \boldsymbol{I}^{(N)}\cdot\boldsymbol{B} - \beta_n g_n^{(C)} \boldsymbol{I}^{(C)}\cdot\boldsymbol{B}, \qquad (1)$$

where $\boldsymbol{S}$, $\boldsymbol{I}^{(C)}$, $\boldsymbol{I}^{(N)}$ are the spin operators of the NV-center (S=1), the ^{13}C atom (I=1/2) and the ^{14}N atom (I=1), respectively. The first term in (1)

$$H_0^{(NV)} = D\left[S_Z^2 - S(S+1)/3\right] + \boldsymbol{S}\cdot A^{(N)}\cdot \boldsymbol{I}^{(N)} + Q\left[(I_Z^{(N)})^2 - I^{(N)}(I^{(N)}+1)/3\right] \qquad (2)$$

describes the NV center in the absence of an external magnetic field and includes the zero-field splitting D~2870 MHz between the m_S =0 and m_S =±1 sublevels of the ground triplet state $^3A_2$ of the center, the *hfi* between the electron spin $\boldsymbol{S}$ and the ^{14}N nuclear spin $I^{(N)}$=1, and the nuclear quadrupole moment of the ^{14}N nucleus. The hyperfine tensor $\boldsymbol{A}^{(N)}$ is diagonal in the principal axis system (PAS) of the NV center, in which the Z axis coincides with the C_{3V} axis of symmetry of the center, while the X and Y axes are chosen arbitrarily, with components $A_{XX}^{(N)} = A_{YY}^{(N)}$ =-2.16 MHz and $A_{ZZ}^{(N)}$ =-2.63MHz. The quadrupole moment of the ^{14}N nuclei is $\boldsymbol{Q}$=-4.95МГц. The second term in the spin-Hamiltonian (1) accounts for the *hfi* between spins $\boldsymbol{S}$ and $\boldsymbol{I}^{(C)}$, described by a matrix $\boldsymbol{A}^{(C)}$, that is generally non-diagonal in the NV PAS. The final three terms in Eq. (1) represent the Zeeman interactions of all three spins $\boldsymbol{S}$, $\boldsymbol{I}^{(C)}$, $\boldsymbol{I}^{(N)}$ with the external magnetic field $\boldsymbol{B}$. Here, β_e = 1.39964 MHz/G and β_n = 0.76226 kHz/G are the Bohr magneton and the nuclear magneton, respectively, $g^{(NV)}$ = 2.0028, $g_n^{(N)}$ = 0.4037607 and $g_n^{(C)}$ = 1.40483 are the g-factors of the NV center, ^{14}N and ^{13}C nuclear spins. In addition to the well-established parameters of the ^{14}NV center [10], we use the *hfi* matrices $\boldsymbol{A}^{(C)}$ obtained from quantum chemical calculations reported in [7].

Using the spin-Hamiltonian (1), we could calculate the energy levels E_α and eigenstates $|\Psi_\alpha\rangle$ of a ^{14}NV – ^{13}C spin system in external magnetic field with given values of the magnitude B and its orientation angles θ, and φ. Typical energy levels and allowed transitions between them for a spin system ^{14}NV-^{13}C in magnetic field $\boldsymbol{B}$ are presented in Fig. 1, where the hyperfine structure due to the nuclear spins ^{14}N and ^{13}C is schematically shown. In particular, the splittings $\boldsymbol{\Delta}^{\pm}$, $\boldsymbol{\Delta}^{\boldsymbol{0}}$ of the NV substates with spin projections m_S=±1,0 arise from the combined effect of the magnetic field and *hfi* with ^{13}C.

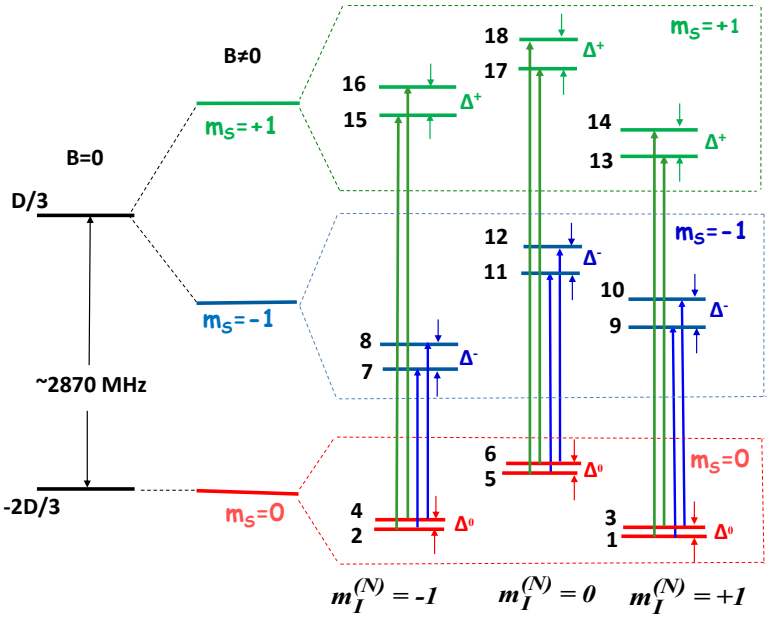


Fig. 1 Hyperfine structure and allowed transitions in a hybrid ^{14}NV –^{13}C spin system subjected to an external magnetic field $\boldsymbol{B}$. The m_S and $m_I^{(N)}$ are projections of the vectors $\boldsymbol{S}$, $\boldsymbol{I}^{(N)}$. The splittings Δ^+, Δ^-, and Δ^0 arise from the combined effects of the magnetic field and hyperfine interaction with the ^{13}C nuclear spin

Of particular importance is the splitting Δ^0 of the m_S=0 sublevels, which depends on the azimuthal angle φ. This dependence is described by an approximate analytical formula [3]

$$\Delta^0 \approx 2\left|\gamma_e B \sin\theta\right| / D\left(\sqrt{A_{XX}^{(C)2} + A_{ZX}^{(C)2}}\cos^2\varphi + \left|A_{YY}^{(C)}\right|\sin^2\varphi\right), \qquad (3)$$

where $\gamma_e = \beta_e g^{(NV)}$ is the gyromagnetic ratio of the NV center and $A_{KL}^{(C)}$ are the components of the matrix describing *hfi* between the NV center and the ^{13}C spin in the specially chosen PAS, where the ^{13}C atom lies in the XZ plane [3]. Experimental measurement of the splitting Δ^0 in the high-resolution ODMR spectra, followed by comparison with theoretical predictions (3), enables the wanted information about the azimuthal angle.

Due to the relatively large dimension (18x18) of the Hamiltonian matrices, their diagonalization is performed numerically. This allows us to determine the transition frequencies $\omega_{\alpha\beta}$ and their amplitudes $P_{\alpha\beta} \sim \left|\langle \Psi_\alpha | S_X | \Psi_\beta \rangle\right|^2$, and construct the corresponding ODMR spectrum $P_{\alpha\beta}(\omega_{\alpha\beta})$ as a set of δ-functions. For comparison with experimental data, the spectrum was broadened by replacing the δ-functions with Lorentzian lines of equal area. The half-widths Γ of the Lorentzians are chosen according to experimental resolution; in the present work, Γ=0.18 MHz. Matching the calculated and experimental ODMR spectra enables determination of the unknown parameters of the external magnetic field.

Experimental ODMR spectra of single ^{14}NV centers and their complexes with isotopic ^{13}C nuclei were obtained using a high-purity single-crystal diamond sample. The sample consisted of a CVD-grown epitaxial layer on an HTHP substrate, optimized for ultralow nitrogen concentration (<50 ppb). The lateral dimensions of the sample were 4 × 4 mm, with a 20 μm thick CVD layer on 300 μm substrate. During growth, conditions were established to form a layer of isolated NV centers at a depth of several micrometers below the surface.

Initialization and readout of the NV spin state were performed using a 532 nm laser with a power of 230 μW. The emitted fluorescence in the 640–750 nm range was detected using a single-photon detector through an immersion objective (NA = 1.4). The photon count rate was approximately 80,000 counts per second. The single-photon nature of emission was confirmed via measurement of the second-order correlation function $g^2(\tau)$.

ODMR measurements were carried out using a home-built setup based on an Integra Spectra 500 confocal microscope. The external magnetic field was generated by permanent magnets, providing both vertical and in-plane components. Microwave control of the NV spin state was achieved using a broadband wire antenna positioned close to the selected NV center, with a microwave power of 0.06 W. ODMR spectra were recorded using a pulsed technique with synchronous signal detection.

Individual NV centers were localized using a coordinate grid on the sample surface. Among them, hybrid NV–^{13}C systems with different relative positions of the ^{13}C nucleus were identified. Identification was performed by analyzing ODMR spectra at zero magnetic field, specifically by measuring hyperfine-induced splittings and comparing them with reference values from [7]. These splittings are characteristic of specific families of equivalent ^{13}C lattice sites. In particular, a system with a zero-field splitting of approximately 13 MHz (Fig. 2b) was identified as corresponding to ^{13}C atoms in the third coordination shell of the NV center, as illustrated schematically in Fig. 2a. One such system was selected for detailed study and used to demonstrate vector magnetometry.

3 Results and discussion

Since the primary focus of this work is the hybrid NV–^{13}C system with a third-shell ^{13}C nuclear spin, we begin by formulating a model for this specific configuration. For this purpose, we use data on the spatial positions of carbon atoms and the corresponding *hfi* matrices obtained in [7] for the cluster $C_{510}[NV^-]H_{252}$. As shown in [7], in this cluster there are six equivalent positions for the ^{13}C atom—C(235), C(239), C(247), C(250), C(271), and C(273) (Fig. 2a)—which exhibit a characteristic zero-field splitting of approximately 13 MHz.

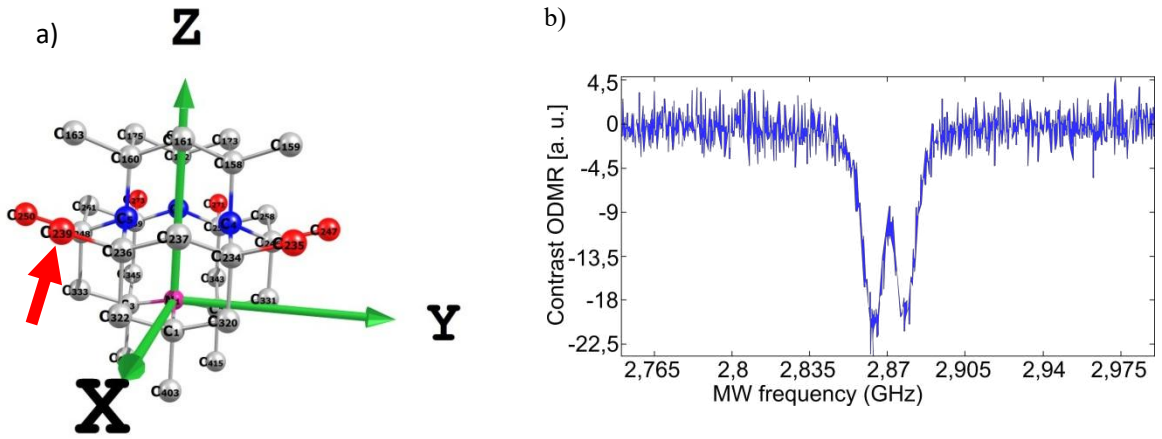


Fig. 2 a) Fragment of the $C_{510}[NV^-]H_{252}$ cluster. Carbon atoms highlighted in red are third neighbors of the NV-center vacancy and exhibit a characteristic zero-field splitting of approximately 13 MHz. The nearest neighbors of the vacancy are shown in blue, and the nitrogen atom of the NV center is shown in purple. The coordinate system used in [7] is also shown; the Z axis is aligned with the NV-center symmetry axis, while the X and Y axes are chosen arbitrarily. **b)** Experimental low-resolution ODMR spectrum of the studied hybrid NV–^{13}C (third-shell) spin system at zero magnetic field, showing the hyperfine-induced zero-field splitting of approximately 13 MHz.

All these positions, highlighted in red in Fig. 2a, correspond to third neighbors of the vacancy of the NV center and are located within the upper sublayer of the diamond bilayer perpendicular to the NV axis (Z axis). Notably, the three nearest neighbors of the vacancy, shown in blue in Fig. 2a and exhibiting the strongest hyperfine interaction with the NV center, are also located in the same sublayer.

In the coordinate system used in [7], the X and Y axes are defined arbitrarily, and therefore the XZ plane does not pass through any of the six third-shell positions. Consequently, the hyperfine matrices reported in [7] cannot be directly used in Eq. (3) for analysis of experimental ODMR spectra. To overcome this, we perform a coordinate transformation such that the selected ^{13}C atom lies in the XZ plane. For definiteness, we consider the position C(239), indicated in Fig. 2a with the red arrow . In the geometry of [7], this atom has coordinates R239= [3.34008 Å, -2.074421 Å, 2.250895 Å] and the corresponding *hfi* matrix for the system NV-^{13}C(239) is of the form (in MHz)

$$\boldsymbol{A}239 = \begin{pmatrix} 13.9404 & -1.9477 & 0.7431 \\ -1.9477 & 14.1884 & -0.9385 \\ 0.7431 & -0.9385 & 12.3735 \end{pmatrix}. \quad (4)$$

By applying a counterclockwise rotation about the Z axis by an angle χ=148.6^0, the XZ plane is aligned to pass through the ^{13}C(239) atom. The hyperfine tensor (4) is then transformed accordingly the standard Z-rotation matrix $\Pi_{(Z\chi)}$ to

$$\bar{A}239 = \Pi_{(Z\chi)}\, A239\, \Pi^{-1}_{(Z\chi)} = \begin{pmatrix} 15.755 & -0.97454 & -1.1264 \\ -0.97454 & 12.373 & 0.4052 \\ -1.1264 & 0.4052 & 12.374 \end{pmatrix}, \quad (5)$$

and used in subsequent numerical calculations based on the spin Hamiltonian (1), as well as in analytical estimates using Eq. (3).

To assess the feasibility of using the ^{14}NV–^{13}C (third-shell) system for vector magnetometry, and to compare it with previously studied first-shell systems [4,5], we first performed test simulations of high-resolution ODMR spectra under the experimental conditions of [5], namely at B=19.3 G, θ=59^0 and φ=71.6^0. The results are shown in Figs. 3, assuming a spectral resolution of Γ =180 kHz. The splitting $\boldsymbol{\Delta^0}$, which is critical for determining the azimuthal angle, is resolved as approximately 0.4 MHz. This value agrees well with the analytical prediction of $\boldsymbol{\Delta^0}$=0.41 MHz obtained from Eq. (3). For comparison, in the first-shell system studied in [5], a significantly larger splitting of 5.3 MHz was observed under similar conditions, albeit with lower spectral resolution Γ=1.2 MHz.

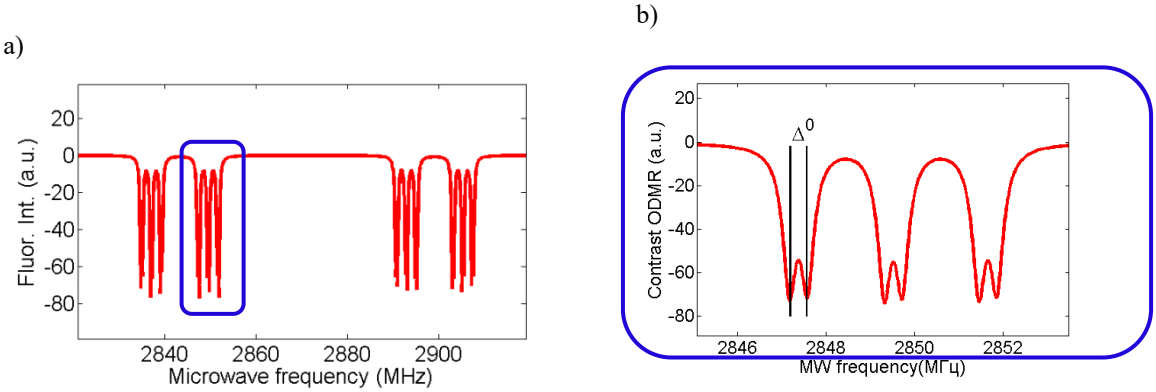


Fig. 3 a) Simulated high-resolution ODMR spectrum of the ^{14}NV-^{13}C(239) complex in an external magnetic field with parameters B=19.3 G, θ=59^0 and φ=71.6^0 , corresponding to the conditions of Ref. [5]. Simulation assume a linewidth of HWHM Γ = 180 kHz. **b**) Enlarged view of the spectral region highlighted by the blue frame in panel **a**).

These results indicate that, given the experimentally achieved resolution of Γ=180 kHz, the ^{14}NV–^{13}C (third-shell) system is suitable for vector magnetometry. Based on this prediction, targeted experiments were carried out to obtain high-resolution ODMR spectra of individual ^{14}NV–^{13}C (third-shell) systems in unknown magnetic fields. Below, we present two such experiments performed on the same hybrid system under different magnetic fields generated by different configurations of permanent magnets around diamond sample.

In both cases, low-resolution ODMR spectra were first recorded using relatively strong microwave power to obtain a coarse overview. An example is shown in Fig. 4, where two broad groups of resonances with a noticeable but poorly resolved structure are observed around 2810 MHz and 2935 MHz. Preliminary analysis using the approach described in [6] yields approximate field parameters B~35 G, θ~47^0. Subsequent high-resolution measurements, performed at much lower microwave power, revealed fine structure within these groups. The part of the Fig. 4 spectrum, similar to that highlighted in Fig. 3 by blue frame, was recorded especially carefully and is presented in Fig. 5 together with its fitting with six Gaussians, which yielded the frequency values of three pairs of peaks: 2809.90 and 2810.51 MHz, 2812.02 and 2812.62 MHz, 2814.22 and 2814.81 MHz. From these experimental data it follows that the

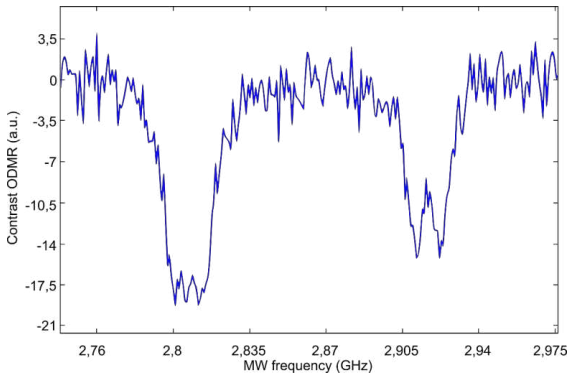


Fig. 4 Low-resolution ODMR experimental spectrum of a single ^{14}NV-^{13}C(third-shell) system in the presence of an unknown external magnetic field

obtained multiple resolved peaks correspond to hyperfine splitting due to the ^{14}N nuclear spin (~2.1 MHz) and an additional splitting Δ^0~600 kHz of the m_S=0 substate, caused by the magnetic field acting on the complex.

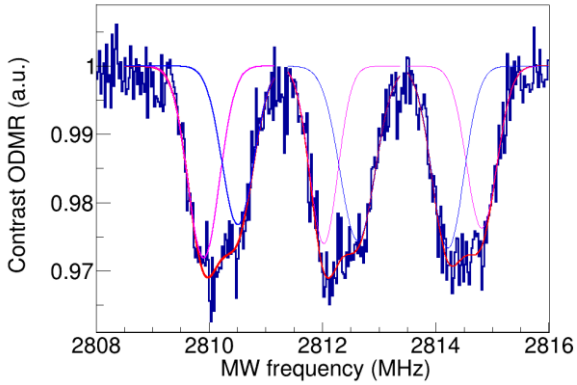


Fig. 5 Enlarged part of the experimentally measured high-resolution ODMR spectrum of a single ^{14}NV–^{13}C (third-shell) complex, together with the result of fitting by six Gaussian components

Numerical simulations of the ODMR spectrum at B = 35 G, θ = 47^0 reproduce this splitting accurately. For example, at φ = 90^0, the calculated value is Δ^0~610 kHz, see Fig. 6a, in good agreement with both the analytical prediction of Eq. 3 (618.7 kHz) and the experimental result (~600 kHz). For comparison, Fig. 6b shows the theoretical prediction of the ODMR spectrum for the ^{14}NV-^{13}C(239) complex in the magnetic field with the characteristics B=35 G, θ=47^0, φ=0^0. In this case, the frequency splitting Δ^0 of two peaks in the simulated spectra is equal to Δ^0=790 kHz. Eq. (3) for this case gives the value Δ^0=789.8 kHz. In addition, the ratio of the amplitudes of these peaks has changed. This example demonstrates that the dependence on the azimuthal angle is significant and can be experimentally measured using this single ^{14}NV-^{13}C complex.

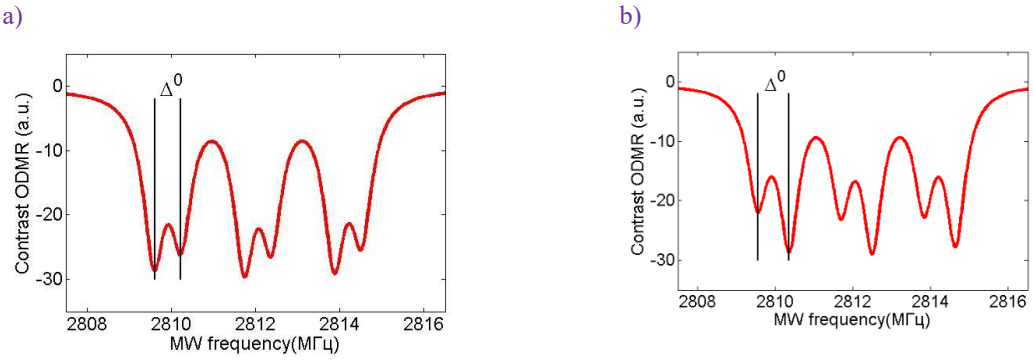


Fig. 6 Theoretically calculated ODMR spectrum of the ^{1}4NV-^{13}C(239) complex in an external magnetic field with B=35 G, θ=47^0: **a**) φ=90^0 ; **b**) φ=0^0

In a second experiment, a stronger magnetic field was applied to the sample by repositioning the permanent magnets. The resulting low-resolution ODMR spectrum exhibited resonance groups near 2866 MHz and 2915 MHz, corresponding to approximate parameters B=72.3 G, θ=84.2^0, i.e., a field nearly perpendicular to the NV axis. High-resolution measurements (Fig. 7) revealed a four-line structure instead of the expected six lines. This is explained by overlap of spectral lines due to the near-coincidence of Δ^0 with the characteristic hyperfine splitting (~2.1 MHz) from the ^{14}N nucleus. Analytical estimates using Eq. (3) confirm that Δ^0 falls within this range for various values of φ, making precise determination of the azimuthal angle challenging in this case. Nevertheless, numerical simulations for different azimuthal angles, shown in Fig. 8, reproduce well the general features of the experimental spectrum.

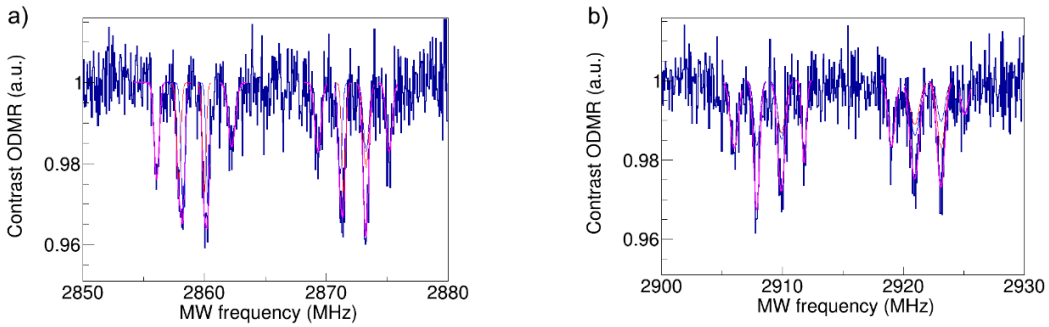


Fig. 7 Experimental high-resolution ODMR spectrum of a single ^{14}NV–^{13}C (third-shell) spin system in the second external magnetic field configuration. Panels **a)** and **b)** show the low- and high-frequency parts of the total spectrum, respectively, together with the results of fitting by 24 Gaussian components

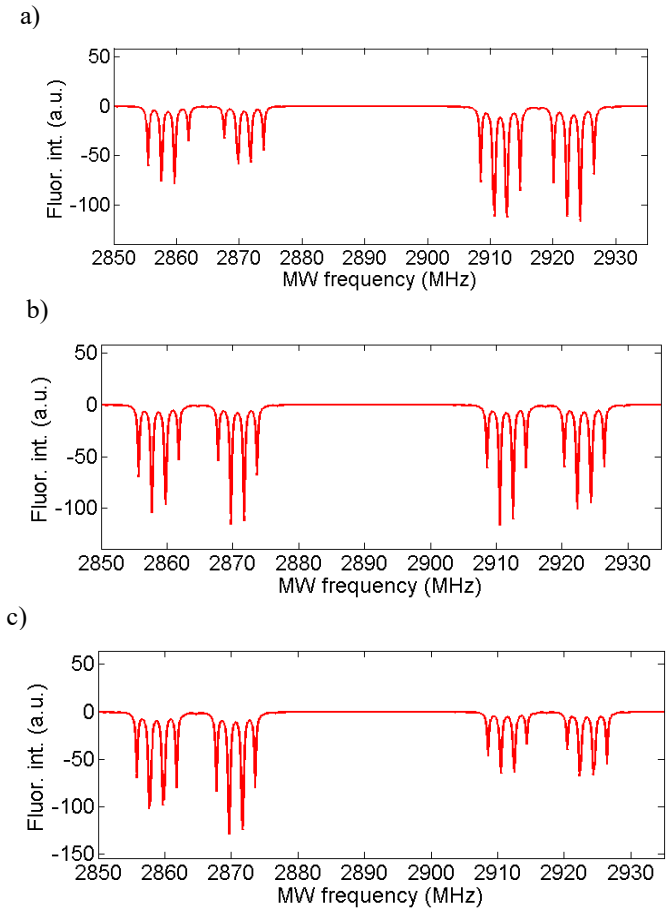


Fig. 8 Numerically simulated ODMR spectra of the ^{14}NV–^{13}C(239) complex in an external magnetic field with B=72.3 G, θ=82.8^0 at different azimuthal angles: **a)** φ=0^0, **b)** φ=45^0, and **c)** φ=90^0

A more detailed comparison was performed by analyzing transition frequencies $\omega_{\alpha\beta}$ and probabilities $P_{\alpha\beta}(\omega_{\alpha\beta})$ for our system ^{14}NV-^{13}C(239). Totally, in this spin system, having 18 energy levels, there can be 18 x 18 = 324 EPR transitions, the probabilities of which, however, differ significantly. Among them, there are transitions having significant probabilities. The frequencies and probabilities of these “strong” transitions in the complex ^{14}NV-^{13}C(239) are shown in blue in Fig. 9 as a bar graph, simulated at B=72.3G, θ=82.3^0, φ=45^0. Simultaneously, we show in red in this figure the frequencies of such lines extracted from the experimental spectrum of Fig. 7 by fitting the spectra with 24 Gaussians. Central frequencies of 24 "strong" lines in these spectra were: 2856.09, 2857.89, 2858.25, 2859.99, 2860.29, 2862.26, 2869.25, 2871.31, 2871.31, 2873.16, 2873.41, 2875.25, 2906.04, 2907.90, 2907.90, 2909.94, 2909.92, 2911.83, 2919.06, 2920.98, 2920.88, 2923.13, 2923.14, 2925.06 MHz.

One can see from Fig. 9 that at azimuthal angle $\varphi = 45^0$, some lines in the ODMR spectrum near-coincide with the experimentally obtained resonances, while the other differ from the experimental ones. Attempts to correct the situation by varying only the azimuthal angle were unsuccessful. The reason is in using in the model standard parameters of the NV center in the Hamiltonian (1) as well as the *hfi* matrices (5), obtained by quantum-chemical simulation for the $C_{510}[NV^-]H_{252}$ cluster [7]. Evidently, improved correspondence can be achieved by introducing small adjustments to these model parameters. Specifically, the best agreement with experimental data (Fig. 10) was obtained for slightly modified magnetic field parameters (B=72.5 G, θ=83.25^0, ϕ=85^0), a reduced zero-field splitting (D=2869.2 MHz), and a scaling factor of 1.12 applied to the hyperfine tensor ($A^{(C)} = 1.12 * \overline{A}239$).

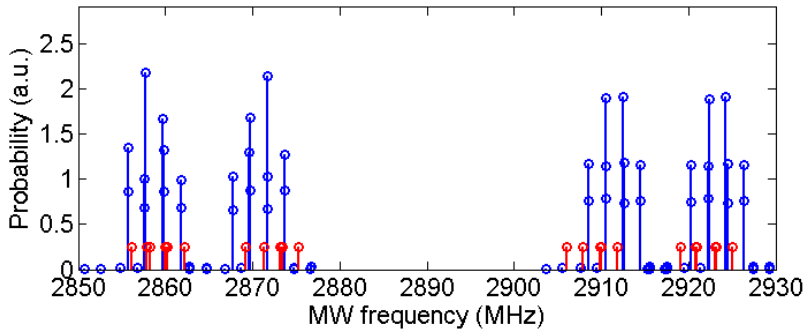


Fig. 9 Calculated transition probabilities and frequencies for the ^{14}NV–^{13}C(239) complex with D=2870 MHz, E=0 MHz, and the hyperfine tensor given by Eq. (5), in a magnetic field with B=72.3 G, θ=82.3^0, φ=45^0. Calculated transitions are shown in blue, while experimentally determined resonance frequencies from the ODMR spectrum in Fig. 7 are shown in red

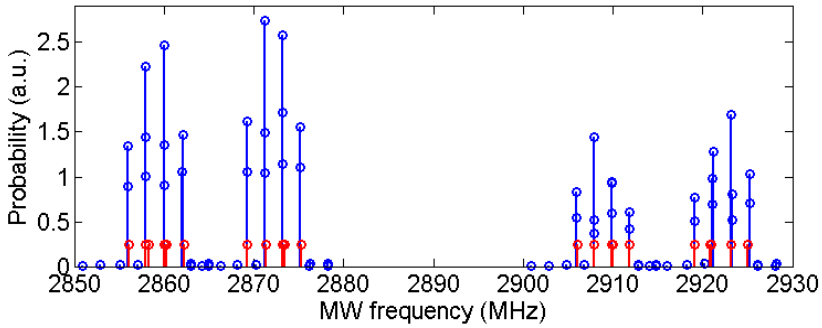


Fig. 10 Calculated transition probabilities and frequencies for the ^{14}NV–^{13}C(239) complex in a magnetic field with B=72.5 G, θ=83.25^0, φ=85^0, using slightly modified values of the hyperfine tensor and the zero-field splitting parameter D as described in the text. Calculated transitions are shown in blue, while experimentally determined resonance frequencies are shown in red

Such adjustments are physically justified, as both the zero-field splitting and hyperfine interaction parameters are known to depend on local environment and temperature [11–14]. Notably, similar scaling (factor 1.02) was previously reported in [15] for low-temperature experiments. The larger factor obtained here likely reflects temperature effects at room conditions. Overall, our results demonstrate that the ^{14}NV–^{13}C (third-shell) system can be effectively used for nanoscale vector magnetometry, although its performance depends on the specific magnetic field configuration and spectral resolution.

4 Conclusion

Using the spin-Hamiltonian formalism, we have simulated high-resolution ODMR spectra of individual hybrid electron–nuclear spin systems (^{14}NV–^{13}C) in diamond in the presence of an external magnetic field. These systems represent promising platforms for nanoscale magnetic field sensing and vector magnetometry with maximal spatial resolution. We have predicted the feasibility of employing for the purpose a ^{14}NV–^{13}C spin system in which the ^{13}C nuclear spin occupies a third-nearest-neighbor position relative to the NV center vacancy. For the first time, high-resolution ODMR spectra of such three-spin system have been experimentally obtained and quantitatively interpreted. This analysis enables determination of both the magnitude and orientation of the local external magnetic field acting on the system.

Acknowledgments We are grateful to V.A. Pushkarchuk for careful reading the manuscript and assistance in its formatting.

Author Contributions A.P.N. performed numerical simulations of the ODMR spectra, prepared the figures of theoretical results, and wrote the main manuscript text. A.L.P. carried out the quantum-chemical calculations. N.S.K., A.R.M., A.K.N., A.A.B., P.A.S., and V.G.S. performed the experimental measurements, processed the data, and prepared the experimental figures. A.N.V. and S.Ya.K. contributed to the interpretation of the results and supervised the work. All authors reviewed the manuscript.

Funding The work was carried out with the financial support of the Ministry of Science and Higher Education of the Russian Federation (agreement on the provision of a grant from the federal budget for the implementation of major scientific projects in priority areas of scientific and technological development No. 075-15-2024-556 dated April 25, 2024).

Data Availability The datasets generated and/or analyzed during the current study are available from the corresponding author on reasonable request.

Declarations

Conflict of Interests The authors declare no competing interests.

Ethics Approval and Consent to Participate Not applicable.

References

1. W.P. Schleich, K.S. Ranade, · Ch. Anton, · M. Arndt et al. Appl. Phys. B, 122, 130 (2016). https://doi.org/10.1007/s00340-016-6353-8.
2. R. Schirhagl, K. Chang, M. Loretz, Ch.L. Degen. Annu. Rev. Phys. Chem., 65, 83 (2014). https://doi.org/10.1146/annurev-physchem-040513-103659.
3. K.R.K. Rao, D. Suter. Phys. Rev. B., 94, 060101(R) (2016). https://doi.org/10.1103/PhysRevB.94.060101.
4. F.-J. Jiang, J.-F.Ye, Z. Jiao, Z.-Y.Huang, H.-J. Lv. Chin. Phys. B., 27, 057601 (2018). https://doi.org/10.1088/1674-1056/27/5/057601.
5. F.-J. Jiang, J.-F.Ye, Z. Jiao, J. Jiang, K. Ma, X.-H.Yan, H.-J. Lv. Chin. Phys. B., 27, 057602 (2018). https://doi.org/10.1088/1674-1056/27/5/057602.
6. A.P. Nizovtsev, N.S. Kukin, A.R. Muradova, P.A. Semenov, A.T. Salkazanov, M.O. Smirnova, A.L. Pushkarchuk,A.N. Vasilev, N.I. Kargin, S.Ya. Kilin. J. Appl. Spec., 89, 1064 (2023). https://doi.org/10.1007/s10812-023-01467-0.
7. A.P. Nizovtsev, S.Ya. Kilin, A.L. Pushkarchuk, V.A. Pushkarchuk, S.A. Kuten, O.A. Zhikol, S. Schmitt, T. Unden, F. Jelezko. New J. Phys., 20, 023022 (2018). https://doi.org/10.1088/1367-2630/aaa910.
8. N. S. Kukin, A. R. Muradova, A. K. Nikitin, A. A. Bukhtiyarov, P. A. Semenov, A. N. Vasil′ev, N. I. Kargin, M. O. Smirnova, S. A. Terent′ev, S. A. Tarelkin, and N. V. Kornilov.Zh. Eksp. Teor. Fiz., 164, 1 (2023), ID:23172, in Russian.
9. N.S. Kukin, A.R. Muradova, A.K.Nikitin, A.A. Buhtijarov, A.P. Nizovtsev, P.A. Semenov, A.N. Vasiliev, N.I. Kargin, M.O. Smirnova. J. Appl. Spec., 90, 1212 (2024). https://doi.org/10.1007/s10812-024-01655-6.
10. T. Xie, Z. Zhao, M. Guo, N. Wang, F. Shi, J. Du. Phys. Rev. Lett., 127, 053601 (2016). https://doi.org/10.1103/PhysRevLett.127.053601.
11. V.M. Acosta, E. Bauch, M.P. Ledbetter, A. Waxman, L.-S. Bouchard, D. Budker. Phys. Rev. Lett. 104, 070801(2010). https://doi.org/10.1103/PhysRevLett.104.070801.
12. M.S.J. Barson, P. Reddy, S. Yang, N.B. Manson, J. Wrachtrup, M.W. Doherty. Phys. Rev. B, 99, 094101 (2019). https://doi.org/10.1103/PhysRevB.99.094101.
13.V.V. Soshenko, V.V. Vorobyov, S.V. Bolshedvorskii, O. Rubinas, I. Cojocaru, B. Kudlatsky, A.I. Zeleneev, V.N. Sorokin, A.N. Smolyaninov, A.V. Akimov. Phys. Rev. B. 102, 125133. (2020). https://doi.org/10.1103/PhysRevB.102.125133.
14. S. Xu, M. Liu, T. Xie, Z. Zhao, Q. Shi, P. Yu, C.-K. Duan, F. Shi, J. Du. Phys. Rev. B.107, L140101 (2023). https://doi.org/10.1103/PhysRevB.107.L140101.
15. M.H. Abobeih,J. Randall, C.E. Bradley, H.P. Bartling, M.A.Bakker, M.J. Degen, M.Markham, D.J. Twitchen, T.H. Taminiau. Nature.576, 411 (2019). https://doi.org/10.1038/s41586-019-1834-7.